Total and Linearly Polarized Synchrotron Emission from Overpressured Magnetized Relativistic Jets

Credit: ESO/M. Kornmesser

Antonio Fuentes

Instituto de Astrofísica de Andalucía (IAA)

J. L. Gómez (IAA), J. M. Martí (UV), M. Perucho (UV)

Polarised Emission from Astrophysical Jets - Ierapetra (Greece), June 12-16 2017

RMHD code (I): Code characteristics

Second-order, conservative, finite-volume, constrained-transport code based on high-resolution shock-capturing techniques.

Code and tests details: **Martí 2015a, 2015b**
State-of-art of numerical RMHD: **Martí and Müller 2015**

Quasi-one-dimensional approximation of the steady-state equations of RMHD (based on **Komissarov et al. 2015**) valid as long as:

- The radial dimension of the flow is much smaller than the axial one: $r \ll z$
- The flow is relativistic in the axial direction: $v^r,\, v^\phi \ll v^z \sim c$
- Consistency with the 1D version of the divergence free condition: $B^r \ll B^\phi,\, B^z$

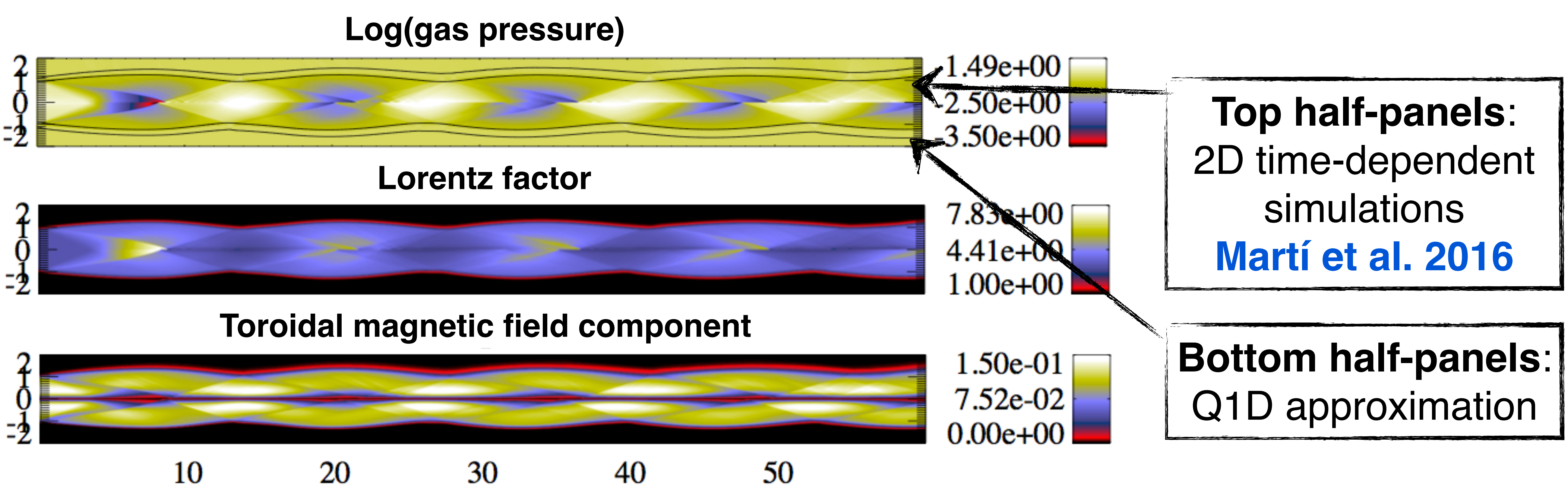

RMHD code (II): Internal structure

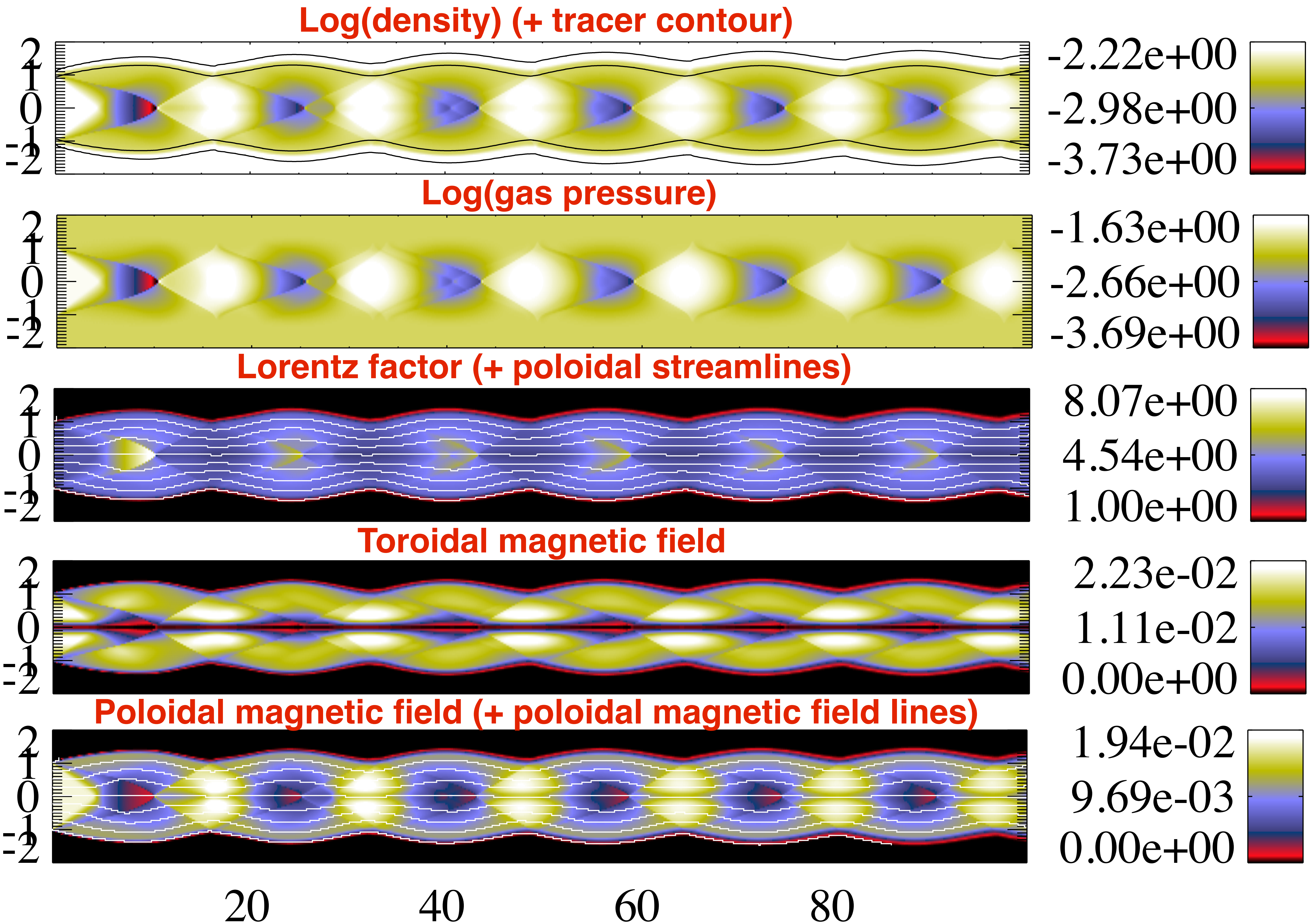

Parameters characterizing the models: $\rho_j,\ v_j,\ K,\ \mathcal{M}_{ms,j},\ \beta_j,\ \phi_j$

RMHD code (III): Parameter space

Magnetosonic Mach number - specific internal energy diagram

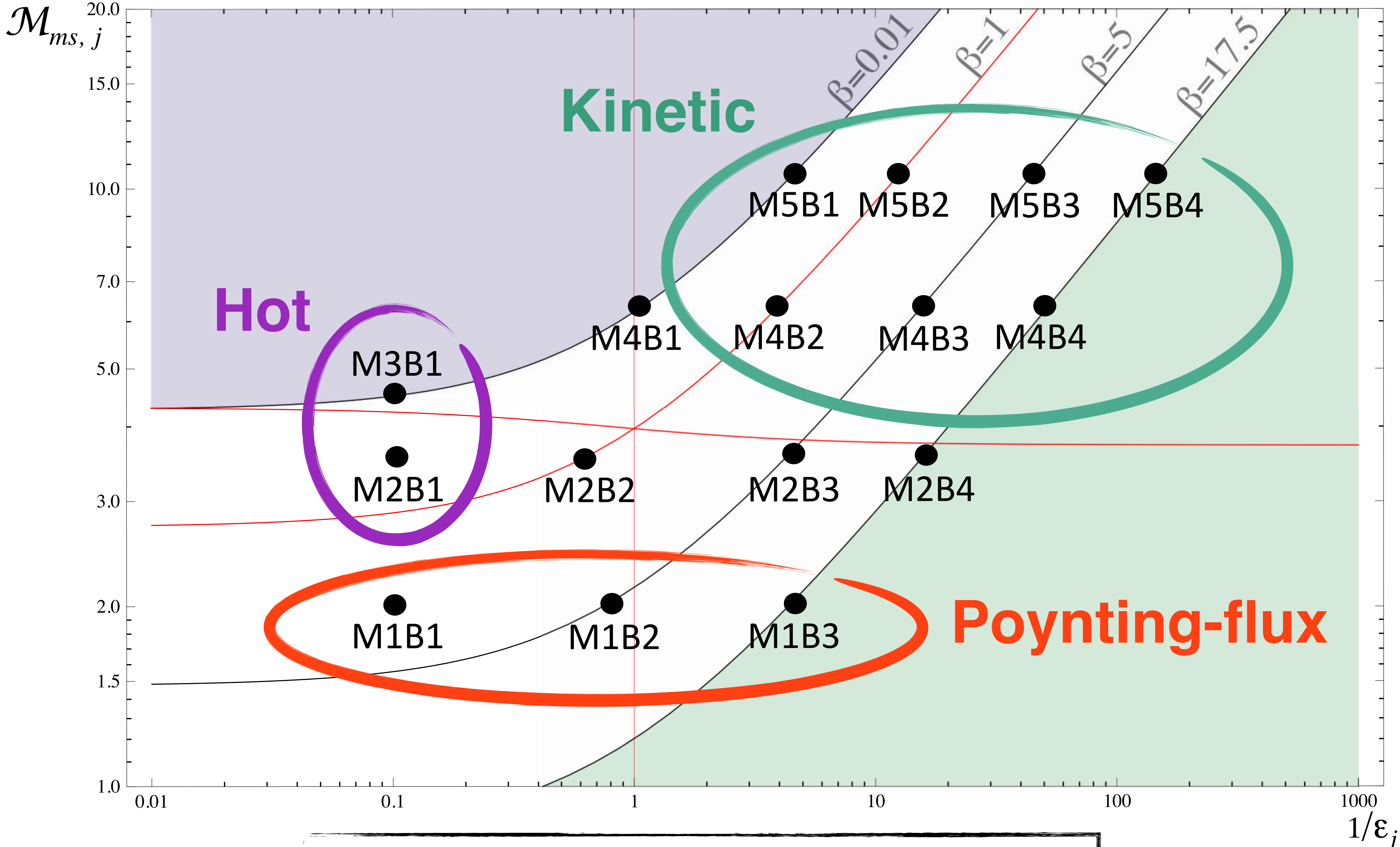

Extending the work presented in Martí et al. 2016

RMHD code (III): Parameter space

Jet models presented in this talk

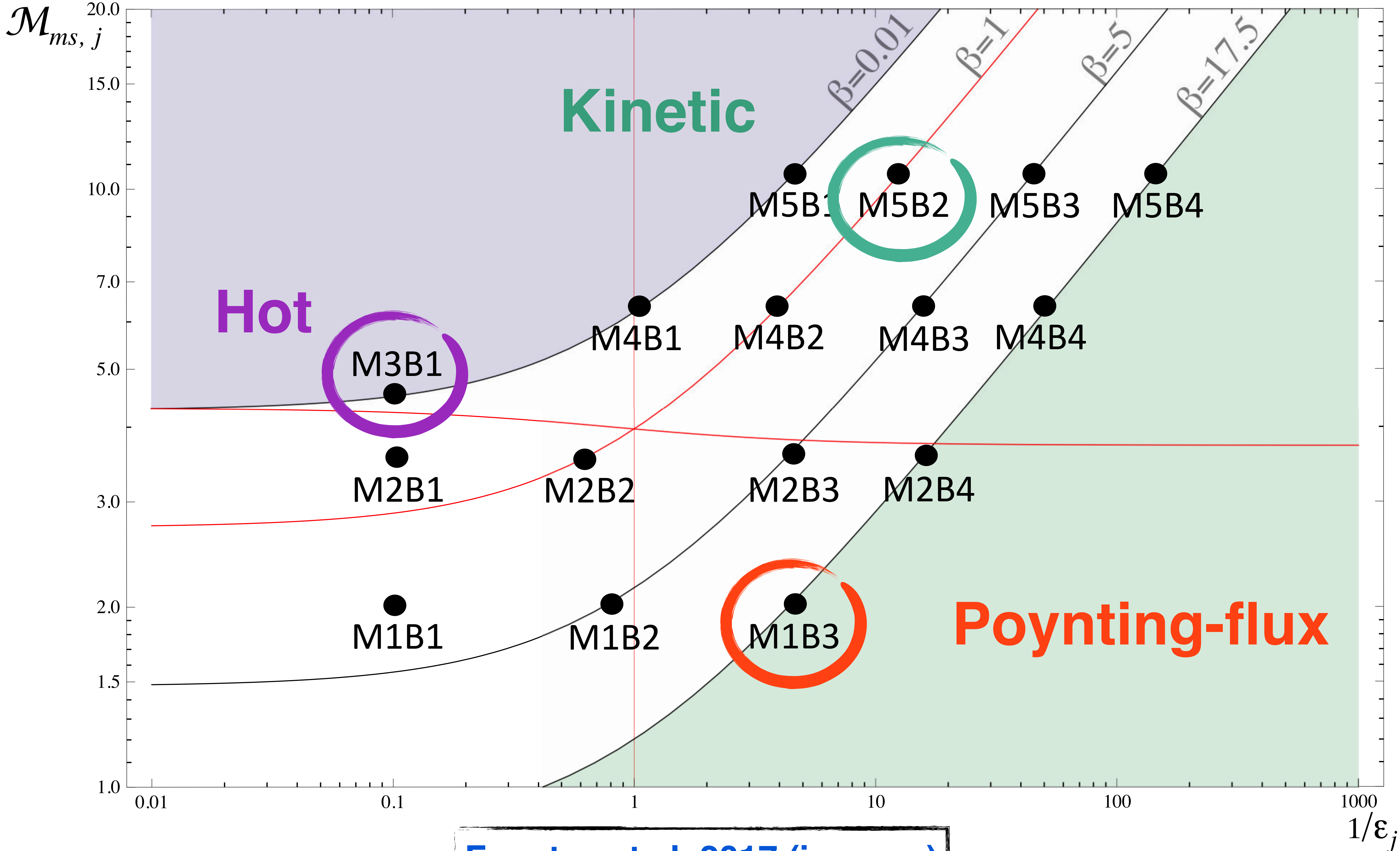

Fuentes et al. 2017 (in prep.)

Radio emission (I): Calculations

Gómez et al. 1995, 1997, 2002

Non-thermal electrons energy distribution: $N(E)\mathrm{d}E = N_0 E^{-\gamma}\mathrm{d}E$

We solve the **transfer equations for synchrotron radiation** (Pacholczyk 1970) **using as inputs the RMHD values**, obtaining the Stokes parameters **I, Q, U (V=0)**

$$\varepsilon^{(i)} = \frac{1}{2} c_5(\gamma) N_o (B\sin\vartheta)^{(\gamma+1)/2} \left(\frac{\nu}{2c_1}\right)^{(1-\gamma)/2} \left[1 \pm \frac{\gamma+1}{\gamma+7/3}\right]$$

$$\kappa^{(i)} = c_6(\gamma) N_o (B\sin\vartheta)^{(\gamma+2)/2} \left(\frac{\nu}{2c_1}\right)^{-(\gamma+4)/2} \left[1 \pm \frac{\gamma+2}{\gamma+10/3}\right]$$

$$\begin{aligned}
\frac{dI^{(a)}}{ds} =& I^{(a)}\left[-\kappa^{(1)}\sin^4\chi_B - \kappa^{(2)}\cos^4\chi_B - \frac{1}{2}\kappa\sin^2 2\chi_B\right] + U\left[\frac{1}{4}(\kappa^{(1)} - \kappa^{(2)})\sin 2\chi_B + \frac{d\chi_F}{ds}\right] \\
& + \varepsilon^{(1)}\sin^2\chi_B + \varepsilon^{(2)}\cos^2\chi_B, \\
\frac{dI^{(b)}}{ds} =& I^{(b)}\left[-\kappa^{(1)}\cos^4\chi_B - \kappa^{(2)}\sin^4\chi_B - \frac{1}{2}\kappa\sin^2 2\chi_B\right] + U\left[\frac{1}{4}(\kappa^{(1)} - \kappa^{(2)})\sin 2\chi_B - \frac{d\chi_F}{ds}\right] \\
& + \varepsilon^{(1)}\cos^2\chi_B + \varepsilon^{(2)}\sin^2\chi_B, \\
\frac{dU}{ds} =& I^{(a)}\left[\frac{1}{2}(\kappa^{(1)} - \kappa^{(2)})\sin 2\chi_B - 2\frac{d\chi_F}{ds}\right] + I^{(b)}\left[\frac{1}{2}(\kappa^{(1)} - \kappa^{(2)})\sin 2\chi_B + 2\frac{d\chi_F}{ds}\right] \\
& - \kappa U - (\varepsilon^{(1)} - \varepsilon^{(2)})\sin 2\chi_B.
\end{aligned}$$

Accounting for **relativistic effects** such as **Lorentz transformations, Doppler boosting** and **light aberration**.

Radio emission (II): Synthetic images

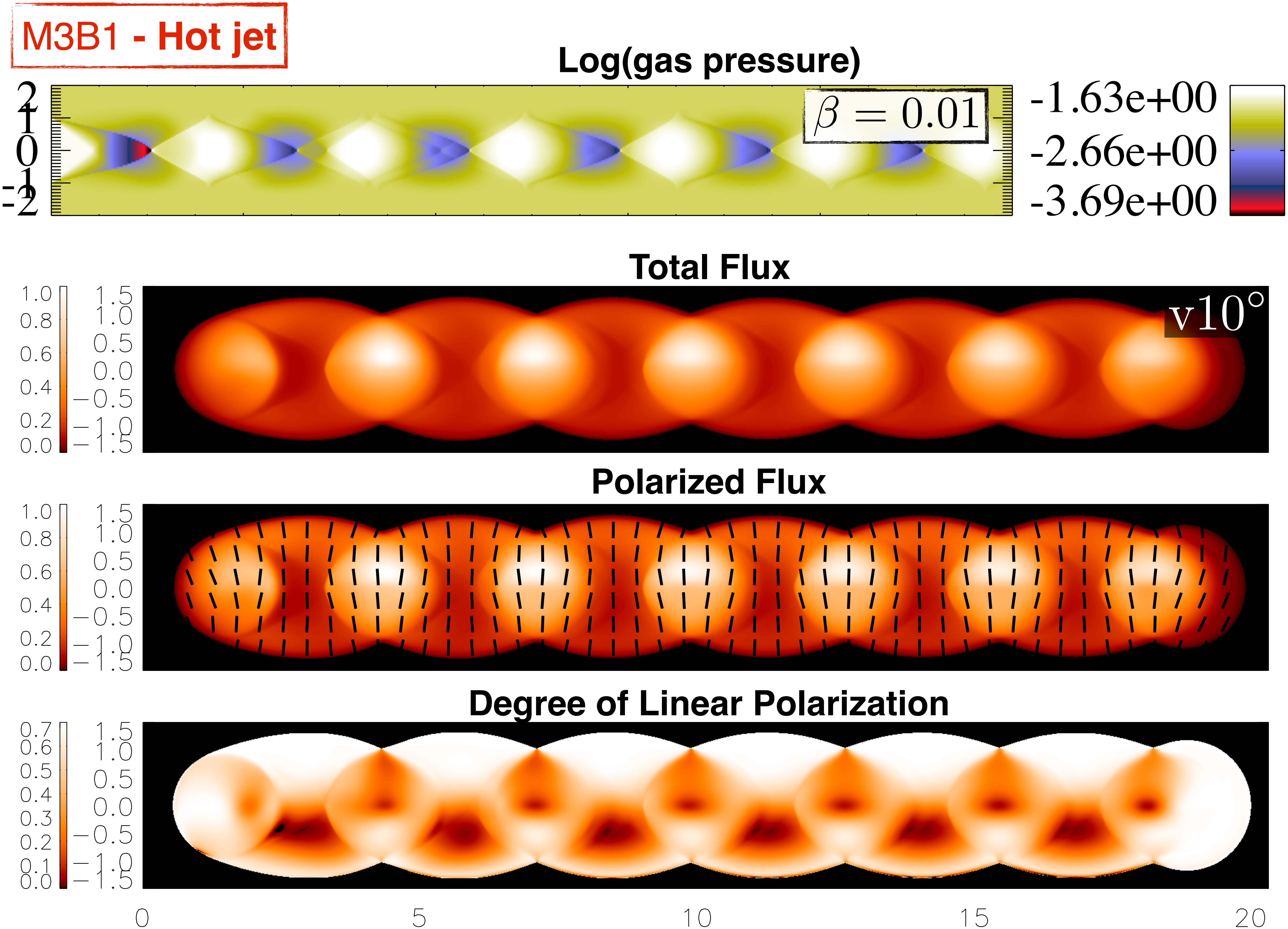

Radio emission (II): Synthetic images

M1B3 - Poyting-flux dominated jet

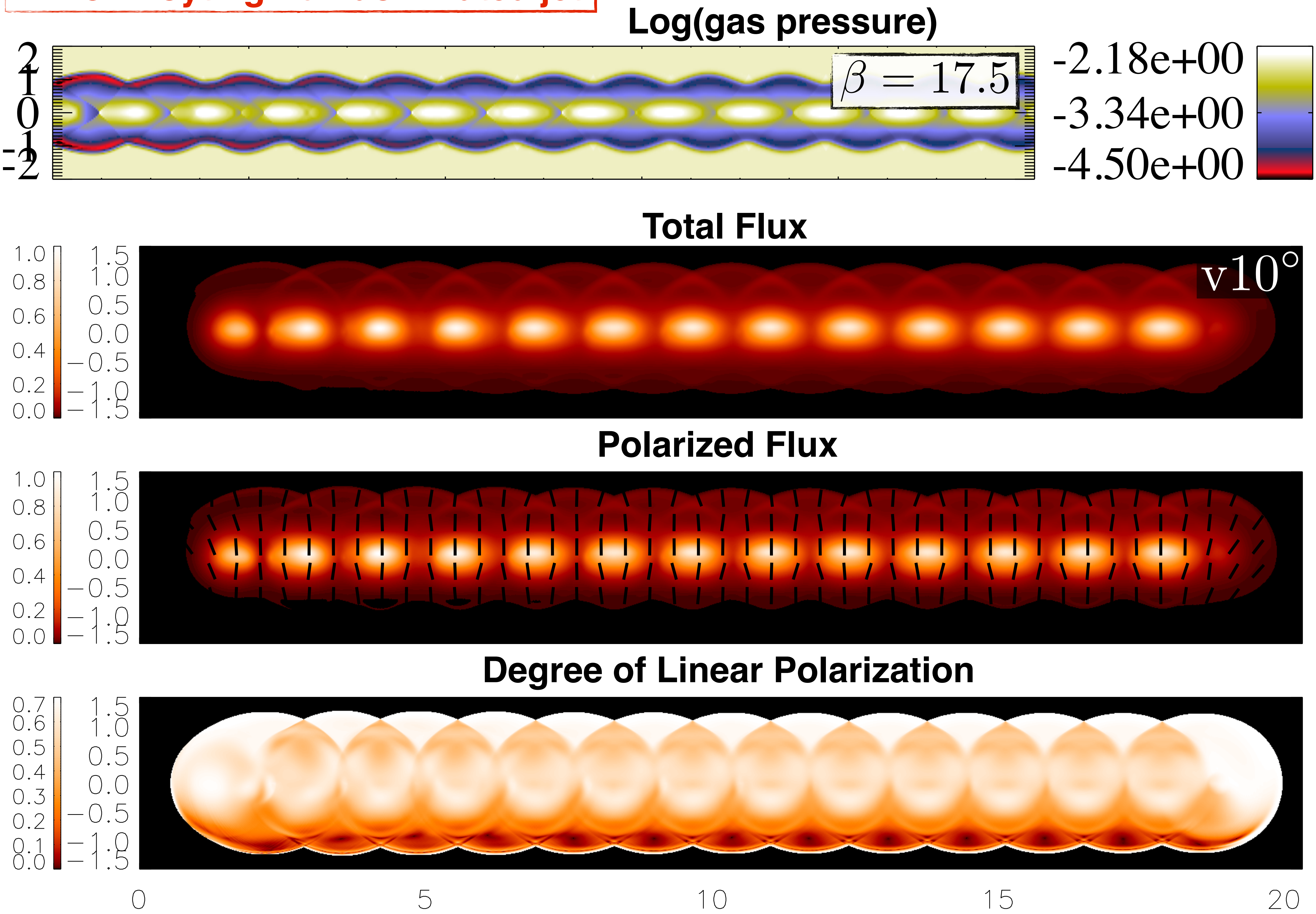

Radio emission (II): Synthetic images

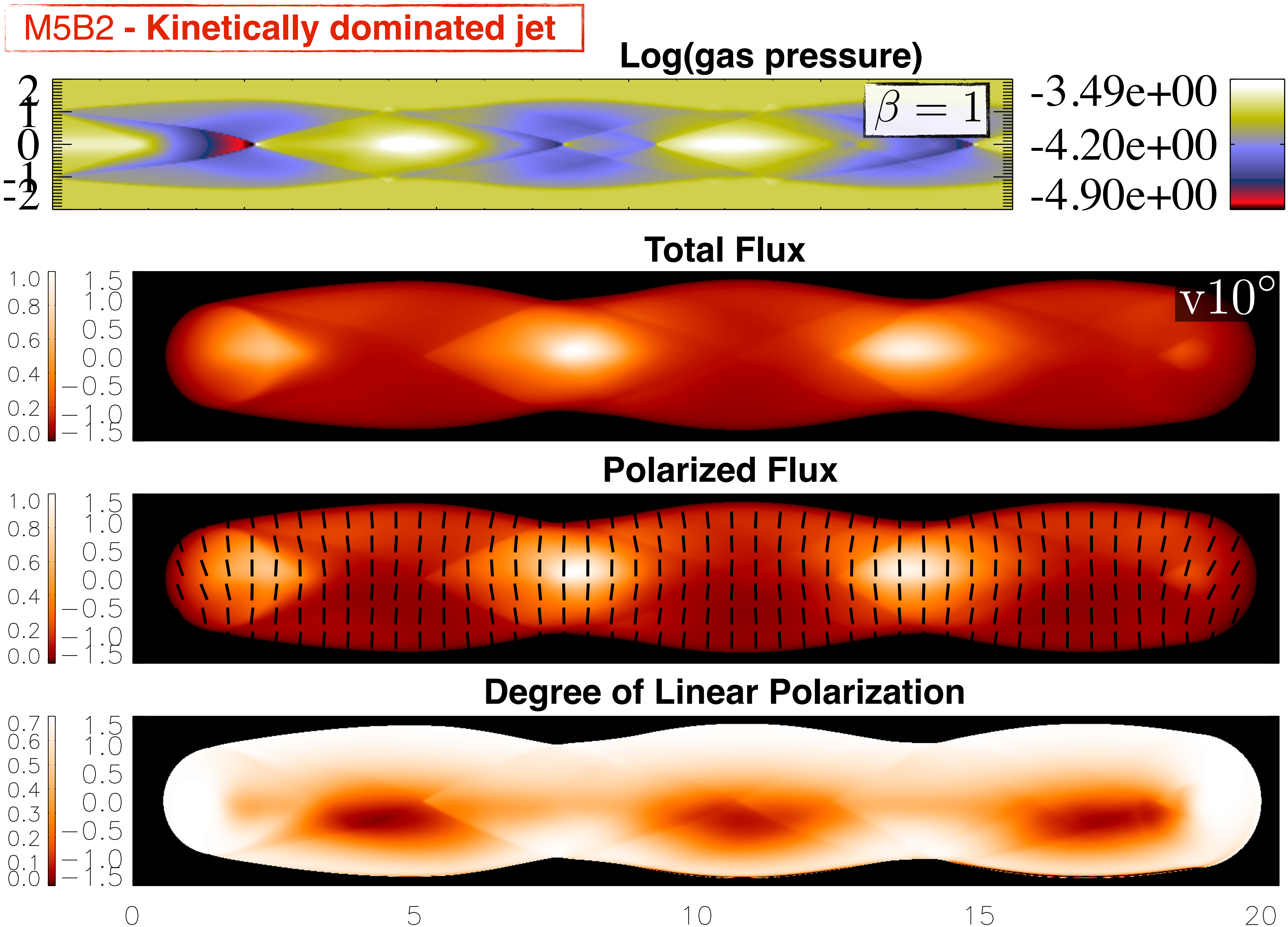

Radio emission (III): Stationary components intensity

Total flux axial profiles

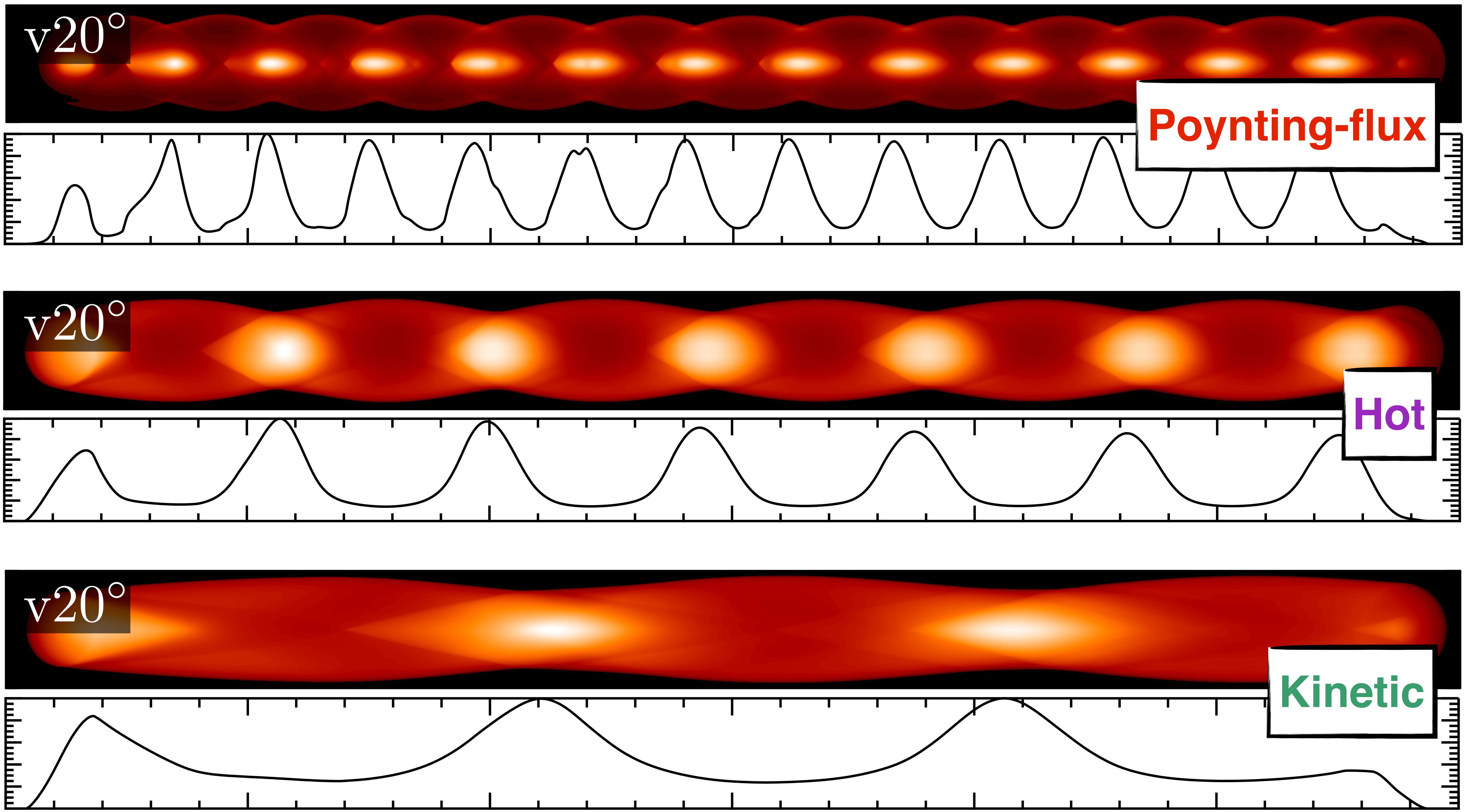

Radio emission (III): Stationary components intensity

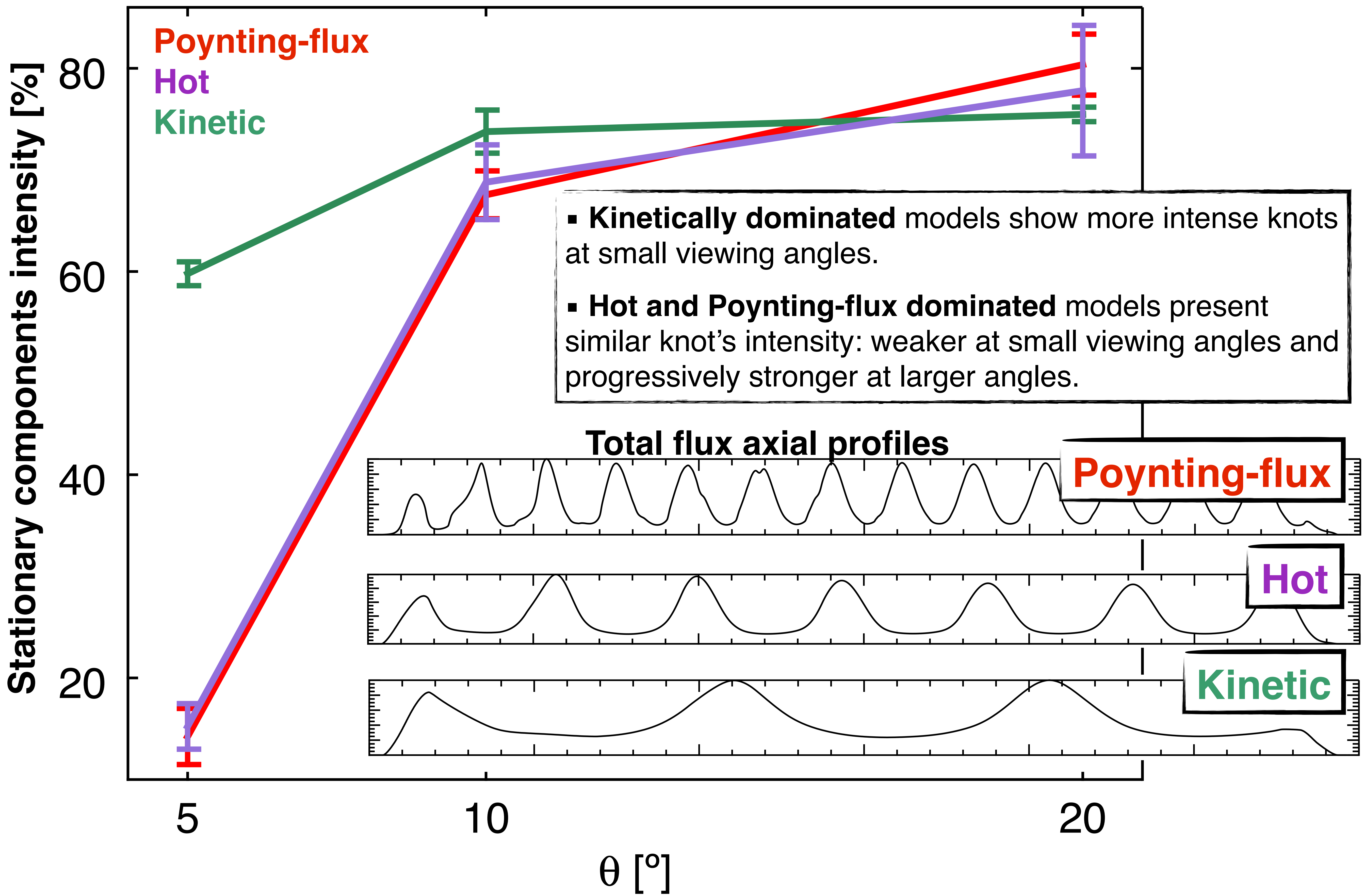

Radio emission (IV): Top-down asymmetry and emission confinement

- Total and polarized **emission asymmetry** between the top and bottom jet halfs due to the **helical magnetic field** structure.
- **Emission confinement** around jet axis with increasing **magnetization**.
- **Polarized emission drops** near jet axis at small viewing angles due to cancellation of the **toroidal magnetic field component**.

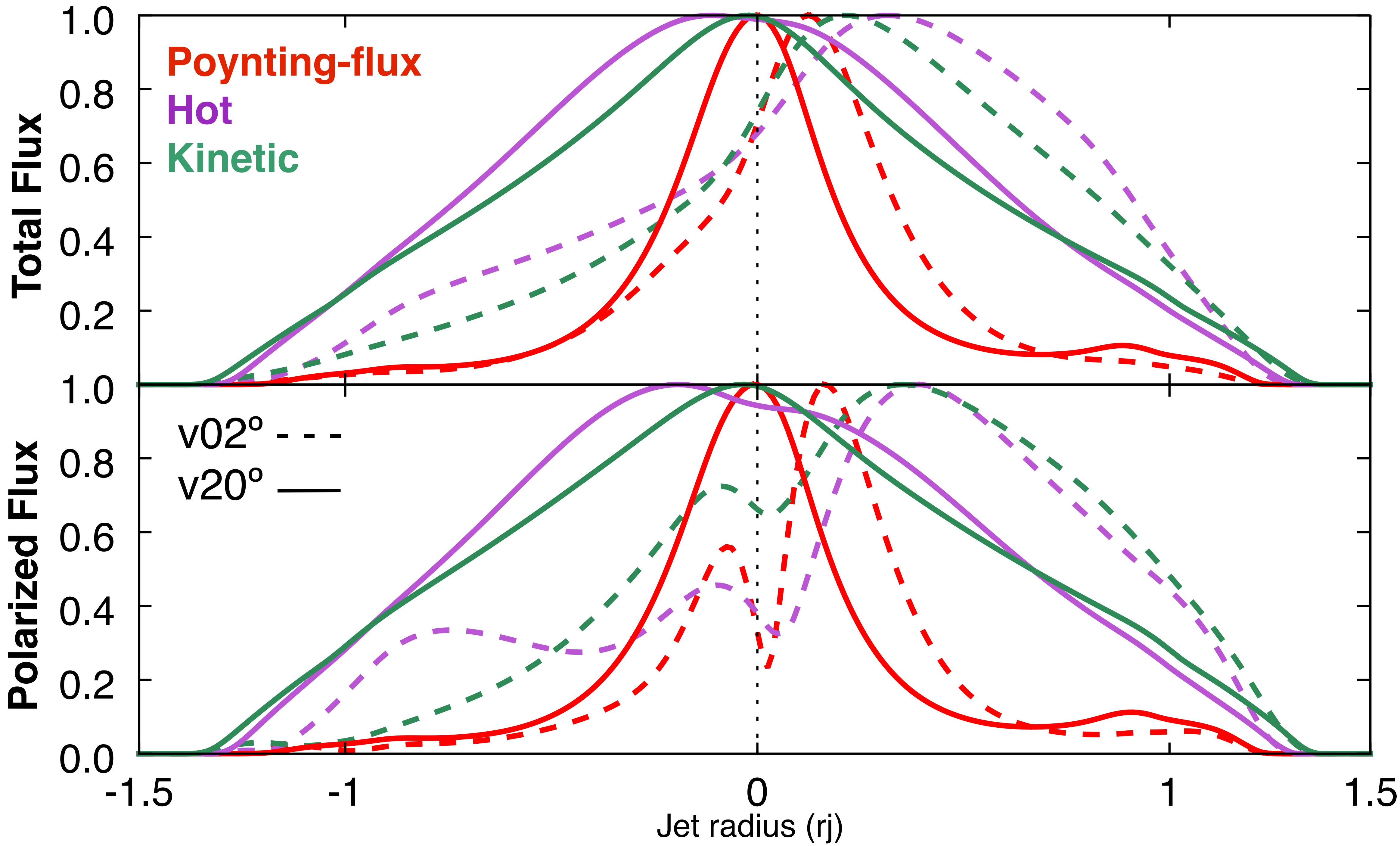

Radio emission (II): Linear polarization and Stokes U asymmetry

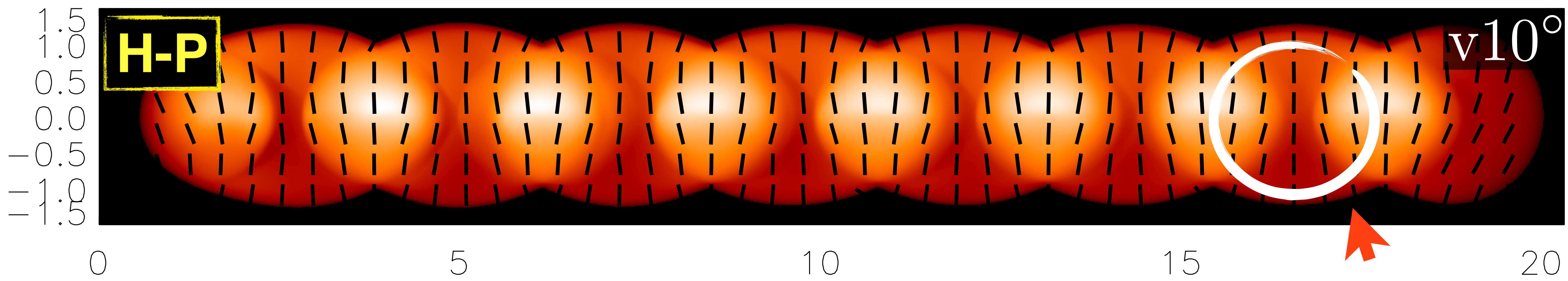

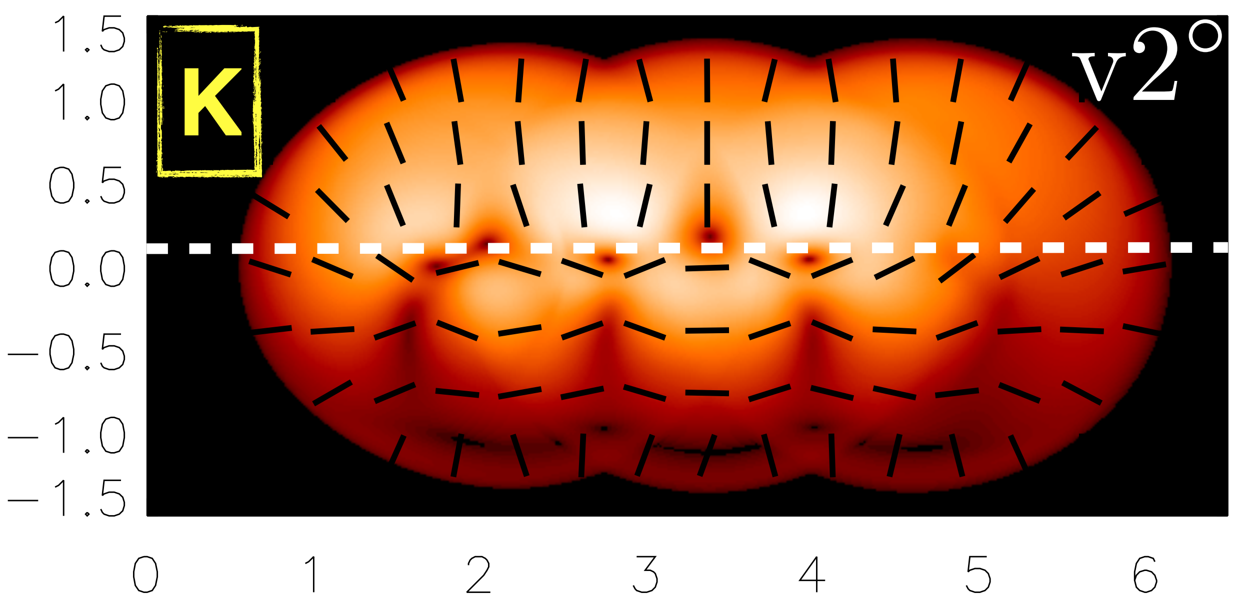

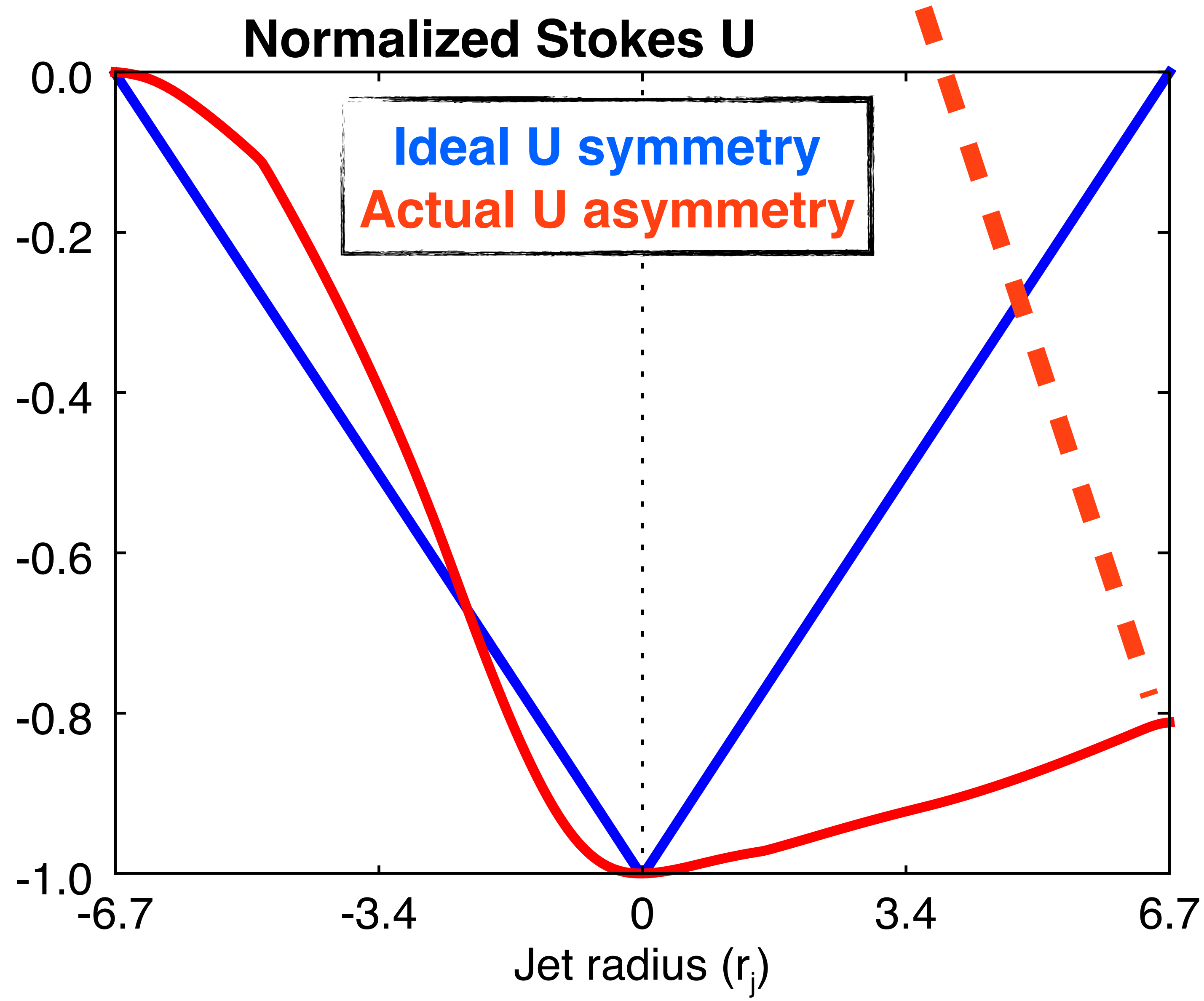

Bimodal distribution of the **EVPAs** at lower angles due to **helical B-field**.

As the **viewing angle increases**, the **EVPAs remain almost perpendicular** to jet axis (poloidal B-field dominates)

Small variations of the **polarization angle (~15º) around stationary components** due to the **break in the Stokes U symmetry**, as a consequence of **recollimation shocks**.

Summary

- We have performed **RMHD simulations** as well as **total and polarized radio emission** of multiple jet models threaded by a **helical magnetic field**, attending to their **dominant type of energy: internal, kinetic or magnetic**.

- The **internal structure** of the models **is determined by the Mach number, the internal energy and the magnetization**.

- **Recollimation shocks** produce **bright stationary components** whose emission gets **confined** in a jet spine as the jet **magnetization increases**. **Kinetic** models show **more intense knots** at **small viewing angles**.

- **Lower viewing angles** show a **bimodal distribution of the EVPAs**, being either perpendicular or aligned with the jet axis. **Small variations in the EVPAs (~15º)** are observed in **recollimation shocks**.